THE JOURNAL OF BIOLOGICAL CHEMISTRY VOL. 289, NO. 18, pp. 12365–12374, May 2, 2014

Characterization of the Testis-specific Proteasome Subunit α4s in Mammals

Received for publication, February 17, 2014, and in revised form, March 19, 2014 Published, JBC Papers in Press, March 25, 2014, DOI 10.1074/jbc.M114.558866

Hiroyuki Uechi, Jun Hamazaki, and Shigeo Murata[1]

From the Laboratory of Protein Metabolism, Graduate School of Pharmaceutical Sciences, The University of Tokyo, 7-3-1 Hongo, Bunkyo-ku, Tokyo 113-0033, Japan

Background: Two subtypes of proteasome core particles (CPs) with tissue-specific β subunits have been identified in mammals.
Results: Mammals have an additional proteasome α subunit, α4s, which forms the male germ-specific CP.
Conclusion: The α4s-containing CP is a new subtype of CP with unique properties distinct from the constitutive CP.
Significance: Our results provide a clue for understanding the role of the proteasome in mammalian testes.

The 26 S proteasome is responsible for regulated proteolysis in eukaryotic cells. It is composed of one 20 S core particle (CP) flanked by one or two 19 S regulatory particles. The CP is composed of seven different α-type subunits (α1-α7) and seven different β-type subunits, three of which are catalytic. Vertebrates encode four additional catalytic β subunits that are expressed predominantly in immune tissues and produce distinct subtypes of CPs particularly well suited for the acquired immune system. In contrast, the diversity of α subunits remains poorly understood. Recently, another α subunit, referred to as α4s, was reported. However, little is known about α4s. Here we provide a detailed characterization of α4s and the α4s-containing CP. α4s is exclusively expressed in germ cells that enter the meiotic prophase and is incorporated into the CP in place of α4. A comparison of structural models revealed that the differences in the primary sequences between α4 and α4s are located on the outer surface of the CP, suggesting that α4s interacts with specific molecules via these unique regions. α4s-containing CPs account for the majority of the CPs in mouse sperm. The catalytic β subunits in the α4s-containing CP are β1, β2, and β5, and immunosubunits are not included in the α4s-containing CP. α4s-containing CPs have a set of peptidase activities almost identical to those of α4-containing CPs. Our results provide a basis for understanding the role of α4s and male germ cell-specific proteasomes in mammals.

The ubiquitin-proteasome system is one of the major routes for intracellular protein degradation in eukaryotes (1). Short-lived proteins and abnormal proteins are tagged with ubiquitin chains and are selectively degraded by the 26 S proteasome. This ATP-dependent protease is involved in a diverse array of biological events, including cell-cycle regulation, DNA repair, immune response, and protein quality control (2, 3).

The molecular composition of the proteasome is well conserved across eukaryotes. The 26 S proteasome consists of a 20 S core particle (CP)[2] and one or two 19 S regulatory particles, which include 14 and 19 different subunits, respectively (4). The CP is composed of seven homologous α subunits (α1-α7) and seven homologous β subunits (β1-β7) that are arranged as a cylinder of four heteroheptameric rings: $\alpha_{1-7}\beta_{1-7}$-$\beta_{1-7}\alpha_{1-7}$ (5). The inner two β rings form a proteolytic chamber, whereas the outer two α rings serve as a gate for substrate entry into the chamber. Of these 14 CP subunits, β1, β2, and β5 have catalytic activities referred to as caspase-like, trypsin-like, and chymotrypsin-like activity, respectively (4). This type of CP is often called the constitutive CP (cCP). The cCP is the basic type of CP and is found from yeast to mammals. In mammals, the cCP is the predominant subtype of CP in most tissues.

Besides β1, β2, and β5, vertebrates have four additional catalytic β subunits, called β1i, β2i, β5i, and β5t. They are incorporated into CPs in the place of their most closely related β subunits, thus forming distinct subtypes of CPs. Two additional subtypes of CPs have been identified up to now. One is the immunoproteasome (iCP), which has β1i, β2i, and β5i as catalytic subunits and is constitutively expressed in lymphoid cells. The expression of iCPs can be induced by interferon γ in non-lymphoid cells. The other is the thymoproteasome (tCP), where β5t is incorporated in place of β5 or β5i together with β1i and β2i. The tCP is found exclusively in cortical thymic epithelium cells. Both iCPs and tCPs have peptidase activities different from those of the cCP that play important roles in their specific functions. The iCP efficiently generates antigenic peptides that bind to the groove of MHC class I molecules. The tCP plays a pivotal role in the positive selection of $CD8^+$ T cells (6–8).

Although the subtypes of catalytic β subunits have been well studied, the diversity of α subunits has remained unclear. A recent study showed that the mammalian testis has an additional α subunit, referred to as α4s (9). However, its function remains unknown. Here, we further characterized the expression pattern of α4s and the composition of α4s-containing CPs in the mouse testis.

EXPERIMENTAL PROCEDURES

Animals—C57BL/6J mice and imprinting control region (ICR) mice were housed in pathogen-free facilities. All experimental protocols described in this study were approved by the Animal Research Committee of the Graduate School of Pharmaceutical Sciences, The University of Tokyo. For synchrony in

[1] To whom correspondence should be addressed: Tel.: 81-3-5841-4803; Fax: 81-3-5841-4805; E-mail: smurata@mol.f.u-tokyo.ac.jp.
[2] The abbreviations used are: CP, core particle; cCP, constitutive core particle; iCP, immunoproteasome; tCP, thymoproteasome; P14, postnatal day 14.

testicular development, male pups were raised as described previously (10).

Quantitative RT-PCR—Total RNAs of adult mouse tissues were isolated using the RNeasy mini kit (Qiagen) and were reverse-transcribed using the SuperScript VILO cDNA synthesis kit (Invitrogen). Quantitative PCR was performed using Universal ProbeLibrary probes (Roche). Primers used were as follows: G6PD, 5′-GAAAGCAGAGTGAGCCCTTC-3′ and 5′-CATAGGAATTACGGGCAAAGA-3′; α4s, 5′-ACCTTTTCCAAGTGGAGTATGC-3′ and 5′-CTATATTAGTTCCTCGAATTCCAACC-3′.

DNA Constructs—The short hairpin sequence targeting α4 was 5′-UGUUGAUGACUAUCCUUGCAUCGGC-3′. Oligonucleotides with a loop sequence (TTCAAGAGA) were cloned into the pMX vector (a gift from T. Kitamura, The University of Tokyo) together with the mouse U6 promoter. cDNAs of mouse α4, mouse α4s, and human α4 were synthesized from total RNA isolated from mouse testes or HeLa cells. cDNA of human α4s was acquired from the SuperScript Human Testis cDNA Library (Invitrogen). PCR was carried out using PrimeSTAR Max DNA polymerase (TaKaRa). An shRNA-resistant mutant of α4 (referred to as α4*) was generated by introducing point mutations into the sequence targeted by the shRNA (A240T and A241C) without changing amino acid sequences. Amplified fragments were subcloned into either the pcDNA3.1 (Invitrogen) or pIRES vector (Clontech) and sequenced for confirmation.

Cell Culture and Transfection—HEK293T cells were cultured under standard conditions. Transfection was performed using Lipofectamine 2000 (Invitrogen). To generate stable cell lines, transformed HEK293T cells were selected with 4 μg/ml puromycin and/or 4 μg/ml blasticidin. siRNAs targeting human α4 and α6 were purchased from Invitrogen and transfected into cells with Lipofectamine RNAi MAX (Invitrogen) at a final concentration of 50 nM. The 25-nucleotide sequences of siRNAs targeting α4 and α6 were as follows: α4, 5′-UGUUGAUGACUAUCCUUGCAUCGGC-3′; α6, 5′-UAUUCAAUUUGAUGAAUCCUGCCCU-3′.

Antibodies—Rabbit polyclonal antibodies against α4, α4s, and PA200 were raised by immunizing the following recombinant proteins with a His_6 tag: mouse α4 (residues 206–248), mouse α4s (residues 208–250), and human PA200 (residues 1729–1828). Antibodies against α1, α2, α3, α5, α6, α7, β1, β2, β3, β5, β1i, β2i, β5i, Rpt6, Rpn8, and Rpn13 have been described previously (8, 11–14). Antibodies for the FLAG epitope, GAPDH, SOX9, Sycp3, and ubiquitin were purchased from Sigma (catalog no. F1804), Abcam (catalog no. ab8245), Millipore (catalog no. AB5535), Santa Cruz Biotechnology (catalog no. sc-74569), and MBL (catalog no. FK2), respectively.

Separation of Sertoli Cells and Germ Cells—Sertoli cells and germ cells were separated by enzymatic digestion as described previously, with minor modifications (15). Decapsulated testes from adult mice were incubated in DMEM (Nacalai) containing 1 mg/ml collagenase (Sigma) and 0.5 mg/ml deoxyribonuclease I for 45 min at 32 °C in a shaking water bath (80 cycles/min). Leydig and interstitial cells were discarded with the supernatant after sedimentation at unit gravity. The sedimented seminiferous tubules were subsequently digested with 2.5 mg/ml trypsin (Invitrogen) for 20 min at 32 °C in a shaking water bath (80 cycles/min). Cell aggregates were suspended with DMEM containing 10% FBS (MP Biochemicals), passed through a nylon mesh (100 μm), and washed three times with DMEM by centrifugation (5 min, 100 × *g*). The cells were plated on a 10-cm dish and cultured in DMEM containing 10% FBS at 37 °C in humidified 5% CO_2 air. Sertoli cells attach to the dish, whereas germ cells do not. 12 h after plating, floating cells were collected as a germ cell-rich fraction. Sertoli cells were cultured further for 4 days to remove the remaining dead germ cells.

Immunoblotting and Immunoprecipitation—Various mouse tissues, prepuberal testes, Sertoli cells, and germ cells were lysed in a buffer containing 50 mM Tris-HCl (pH 7.5), 5 mM EDTA, 10 mM 2-mercaptoethanol, and 1% SDS for immunoblotting. HEK293T cells, adult mouse testes, and sperm from cauda epididymis were homogenized in an ice-cold buffer containing 25 mM Tris-HCl (pH 7.5), 0.2% Nonidet P-40, 1 mM dithiothreitol, 2 mM ATP, and 5 mM $MgCl_2$ for immunoblotting, immunoprecipitation, and glycerol density gradient centrifugation analysis. For immunoprecipitation of proteasomes, anti-α6 or anti-α4s antibodies bound to protein G-Sepharose (GE Healthcare) were used. Homogenates or lysates were clarified by centrifugation at 20,000 × *g* for 10 min, separated by SDS-PAGE, transferred to a PVDF membrane, and subjected to immunoblot analysis.

Assay of Proteasome Activity—Clarified lysates were subjected to 8–32% (v/v) liner glycerol density gradient centrifugation (22 h and 83,000 × *g*) and separated into 32 fractions, followed by measurement of peptidase activities of each fraction using succinyl-LLVY-7-amino-4-methylcoumarin (Suc-LLVY-MCA) for chymotrypsin-like activity, *t*-butyloxycarbonyl-LRR-MCA for trypsin-like activity, and *N*-benzyloxycarbonyl-LLE-MCA for caspase-like activity, as described previously (8). Ornithine decarboxylase degradation activity was measured as described previously (8).

Immunohistochemistry—Mouse testes were fixed in 4% paraformaldehyde in PBS overnight at 4 °C, dehydrated, and embedded in paraffin. Sections (5 μm thick) were deparaffinized, boiled in 10 mM citrate buffer (pH 6.0), washed in Tris-buffered saline with 0.05% Tween 20 (TBST), and incubated in TBST with 1% goat serum (blocking buffer) for 1 h at room temperature. The sections were then incubated with primary antibodies in blocking buffer overnight at 4 °C. The sections were washed in TBST, incubated with secondary antibodies (Alexa Fluor 488 goat anti-rabbit IgG and Alexa Fluor 594 goat anti-mouse IgG, Invitrogen) in blocking buffer. DAPI staining was performed before sections were mounted with SlowFade (Invitrogen). Images were captured on DMI6000B (Leica). Preimmune serum was used as a negative control. Stages of seminiferous tubule cross-sections were assessed by observing the population of germ cells (16).

Inhibition of Sperm Proteasomes—For inhibition of sperm proteasomes, mouse sperm was incubated in human tubal fluid medium (Millipore) containing 10 μM epoxomicin (Peptide Institute) at 37 °C in humidified 5% CO_2 air.

RESULTS

Identification of a New α-type Subunit with High Homology to α4 in Mammals—In eukaryotic cells, the proteasome contains seven types of α subunits, called α1-α7. Recent progress in whole genome sequencing has uncovered the possible existence of a new gene that encodes a protein with high homology to α subunits in the mammalian genome. These genes have been annotated as *PSMA8* (Gene ID 143471) and *Psma8* (Gene ID 73677) in humans and mice, respectively.

A dendrogram analysis of the gene product of *Psma8*, which has been designated α4s (9), showed the highest homology to α4 (Fig. 1*A*). α4s shares 85% amino acid identity and 94% similarity to α4. Alignments of mouse α4 and α4s peptide sequences revealed that the differences were concentrated in two regions that encompass residues 178–191 and C-terminal residues 219–248 of α4 (Fig. 1*B*, *underlined* in *orange* and *red*), whereas other regions are almost identical.

To predict where these two unique regions locate in the CPs, residues comprising these regions were highlighted in the crystal structural model of the bovine CP (Fig. 1*C*) (17). The unique regions of α4 (Fig. 1*C*, depicted in *orange* and *red*, corresponding to sequences underlined with the same colors in Fig. 1*B*) were located on the outer surface of the CP and do not come into contact with the adjacent subunits, whereas the conserved regions (*blue*) shaped the surfaces that faced the adjacent subunits.

We also predicted the structural models of mouse α4 and α4s by SWISS-MODEL (Fig. 1*D*) (18). A large part of the surfaces generated by the unique regions of α4 and α4s is negatively charged. Because several N- and C-terminal residues of α4 and α4s were not included when the models were generated, we were unable to compare the whole C-terminal unique regions in detail, but a remarkable difference is that the C-terminal unique regions (Glu-223 for α4 and Lys-225 for α4s) have an opposite charge (Fig. 1*D*, *arrowheads*).

Taken together, differences in amino acid sequences between α4 and α4s do not seem to affect CP assembly because the difference is concentrated on the outer surface of the subunits. Rather, it is possible that incorporation of α4s in place of α4 affects interaction of the CP with other, still unidentified molecules.

α4s Is Incorporated into the CP in the Mouse Testis—To examine where α4s is expressed in the mammalian body, we performed a quantitative RT-PCR analysis using various mouse tissues. This revealed that α4s mRNA was specifically expressed in the testis (Fig. 2*A*, *top panel*). We next raised antibodies specific to either α4 or α4s and used them for immunoblotting of mouse tissue extracts. Although α4 protein was expressed in all organs examined, α4s protein was detected exclusively in the testis (Fig. 2*A*, *bottom panel*).

We then asked whether α4s was incorporated specifically into the proteasome in the testis. Lysates from mouse testes were fractionated by glycerol gradient centrifugation, followed by measurement of proteasome activity and immunoblotting of each fraction. 26 S proteasomes and 20 S CPs were sedimented around fractions 24 and 17, respectively. The distribution of α4s coincided with the proteasome activity, just like that of α4, suggesting that α4s is incorporated into the CP in the testis (Fig. 2*B*).

To verify the incorporation of α4s into the CP and to examine the composition of α4s-contaning proteasomes, mouse testis lysates were immunoprecipitated using anti-α6 and anti-α4s antibodies. α6 is an invariable CP subunit, and, therefore, anti-α6 antibody precipitates all subtypes of the CP as well as the 26 S proteasome. Indeed, the composition of the proteasome immunoprecipitates by the anti-α6 antibody was similar to that of the testis lysate. They contained all α subunits, including α4s, and also catalytic subunits of iCPs, β1i, β2i, and β5i (Fig. 2*C*). This is consistent with a previous report showing that the mammalian testis expresses iCP (9). When the testis lysate was immunoprecipitated with anti-α4s antibody, α4 was completely absent from the precipitates (Fig. 2*C*). These results indicate that incorporation of α4 and α4s into the CP is mutually exclusive and that α4s is incorporated into the CP in place of α4. Also, catalytic subunits of iCPs were not observed in α4s-containing proteasomes, indicating that catalytic subunits of the α4s-containing proteasome are the constitutive catalytic subunits β1, β2, and β5 (Fig. 2*C*).

Both of the immunoprecipitates contained regulatory particle subunits (Rpt6, Rpn8, and Rpn13) and PA200, which is a CP activator highly expressed in the mammalian testis (Fig. 2*C*) (19). The relative amounts of these subunits to CP subunits were almost equivalent between the two precipitates, suggesting that there is no significant difference in the affinity for the regulatory particle or PA200 between the α4-containing CP and the α4s-containing CP.

α4s Is Incorporated into the CP in Place of α4—To confirm incorporation of α4s into the CP in place of α4, we next examined how the expression of α4s affects incorporation of α4 into the CP using HEK293T cells, which express cCPs but do not express α4s. To this end, we established cells stably expressing α4s with a C-terminal FLAG tag.

Expression of α4s-FLAG slightly decreased the amount of α4 compared with control cells that did not express α4s-FLAG (Fig. 3, *lanes 1* and *2*). Knockdown of α4 by siRNA decreased CP subunits in control cells, probably because of the defect in CP biogenesis in the absence of α4 (Fig. 3, *lane 3*). In contrast, the decrease in CP subunits by α4 knockdown was modest in α4s-FLAG expressing cells, and the protein level of α4s-FLAG was increased markedly compared with that without treatment of α4 siRNA (Fig. 3, compare *lane 4* to *lane 2*). These observations were specific to α4 knockdown, as revealed by the observation that α6 knockdown did not increase the expression of α4s-FLAG and that expression of α4s-FLAG did not increase CP levels in the absence of α6 (Fig. 3, *lanes 5* and *6*). These results indicate that α4s is a CP subunit that is incorporated in place of α4 during CP biogenesis.

Incorporation of α4s Does Not Alter Proteasome Activities—The two well known subtypes of CPs, the iCP and the tCP, have different catalytic β subunits that confer catalytic activities different from those of the cCP (4). We asked whether α4s-containing CPs have altered peptidase activities. To examine catalytic activities of α4s-containing proteasomes, we established a HEK293T-derived cell line expressing α4s-FLAG. To increase the incorporation of α4s into the CP, a shRNA targeting α4

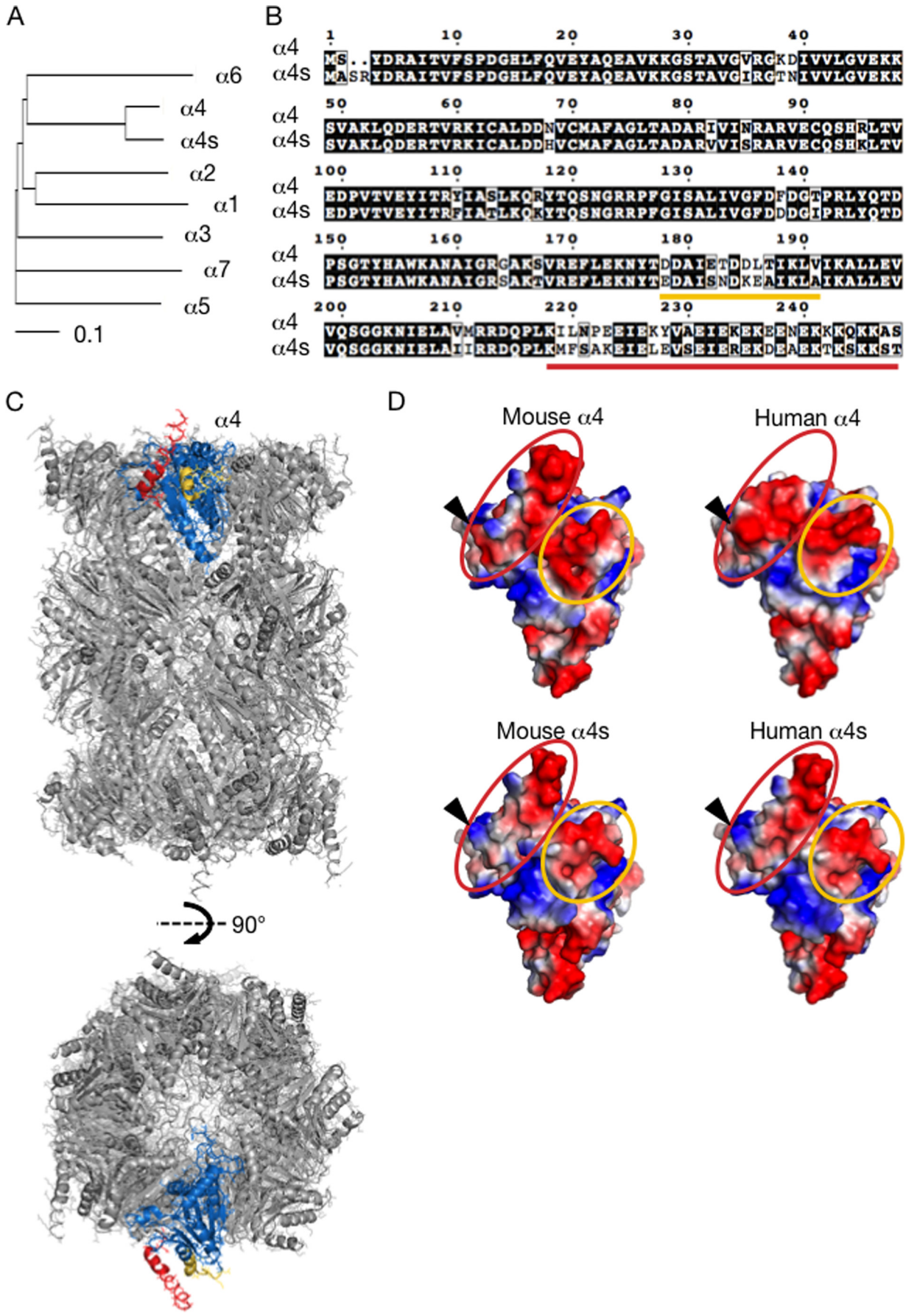
A
α6
α4
α4s
α2
α1
α3
α7
α5
0.1
B
α4
α4s
C
α4
90°
D
Mouse α4
Human α4
Mouse α4s
Human α4s

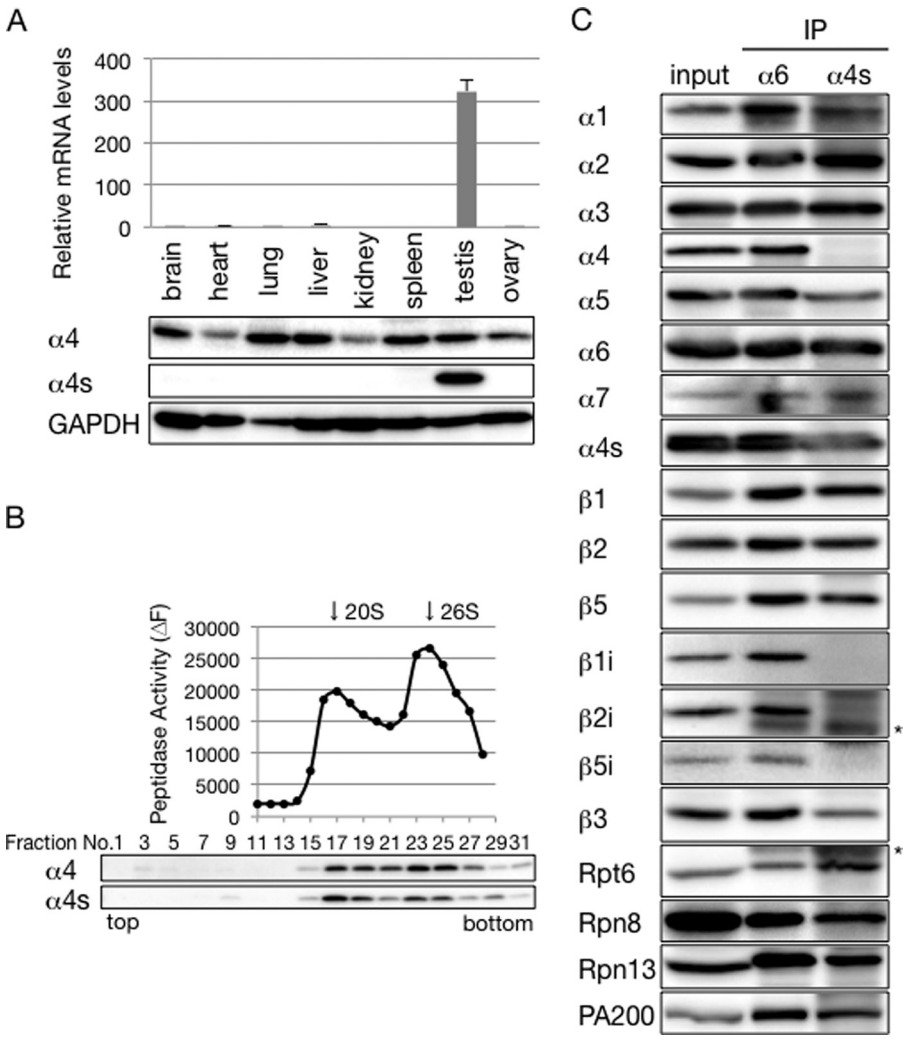

FIGURE 2. **α4s is incorporated into the CP in place of α4 in the mouse testis.** *A*, *top panel*, qRT-PCR analysis of various mouse tissues. α4s mRNA levels were normalized by G6PD mRNA levels. Data are mean ± S.D. ($n = 3$). *Bottom panel*, immunoblot analysis with anti-α4 and anti-α4s antibodies. *B*, extracts of mouse testes were fractionated into 32 fractions by glycerol gradient centrifugation. The chymotrypsin-like activity of the resultant fractions was measured in the presence of 0.025% SDS (*top panel*). *Arrows* indicate the peak locations of the 20 S CP and the 26 S proteasome. Each fraction was subjected to immunoblotting with the indicated antibodies (*bottom panel*). *C*, extracts of mouse testes were immunoprecipitated with anti-α6 antibody or anti-α4s antibody. The immunoprecipitates and input (20%) were subjected to immunoblotting with the indicated antibodies. The *asterisks* denote IgG. Data are representative of three independent experiments (*B* and *C*).

(α4-shRNA) was also stably expressed in the cell line (hereafter referred to as α4s-FLAG cell). As a control, we prepared a cell line stably expressing both α4-shRNA and α4*-FLAG (α4*-FLAG cell). α4*-FLAG encodes an α4-FLAG protein but has synonymous mutations in its DNA sequences targeted by α4-shRNA so that its expression is not affected by α4-shRNA.

Lysates of these two cell lines as well as parental HEK293T cells (mock) were separated by glycerol gradient centrifugation. Immunoblot analysis of the fractions by α6 and Rpt6 showed the locations of 20 S CPs and 26 S proteasomes around fractions 15 and 25, respectively (Fig. 4*A*). The distribution of α4s-FLAG was similar to that of α6, and α4s-FLAG was hardly detected in the lighter fractions (fractions 2–12), confirming that α4s-FLAG was efficiently incorporated into CPs in the α4s-FLAG cells (Fig. 4*A*).

We next measured three known catalytic activities of the proteasome: chymotrypsin-like, caspase-like, and trypsin-like activities. All three peptidase activities in the 20 S CP and 26 S proteasome fractions showed no significant differences between the three cell lines (Fig. 4*B*). Fractions 15 and 25, which correspond to the peak fractions of the 20 S CP and the 26 S proteasome, respectively, were subjected to immunoblot anal-

FIGURE 1. **α4s has high homology with α4.** *A*, dendrogram analysis of mouse α subunits. Data were analyzed using the ClustalW program. *B*, mouse α4 and α4s were aligned using the ClustalW program and visualized by ESPript version 3.06. Identical residues are *boxed* in *black*, and similar residues are written in a *white box*. Two *colored lines* (*orange* and *red*) indicate regions in which differences between α4 and α4s are concentrated. *C*, the unique regions highlighted in the structural model of the bovine 20 S CP. Front (*top panel*) and 90° rotated (*bottom panel*) views (PDB code 1IRU). The unique regions of α4 are shown in the same colors as in *B*, whereas the conserved regions are colored in *blue*. *D*, comparison of the predicted structures of α4 and α4s. The following residues were used for prediction of structural models of mouse and human α4 and α4s by SWISS-MODEL: mouse α4 (2–239), mouse α4s (5–240), human α4 (2–232), and human α4s (5–240). Electrostatic surface potentials (*blue*, positive charge; *red*, negative charge) were visualized by PyMOL. Residues corresponding to the *underlined* amino acid sequences in *B* are surrounded by the same color. The *arrowheads* indicate Glu-223 in α4 and Lys-225 in α4s.

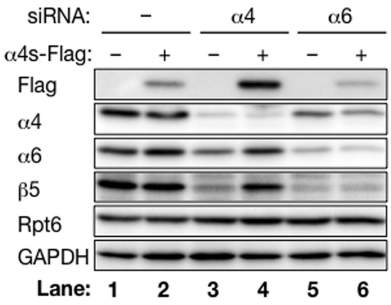

FIGURE 3. **α4s is incorporated into the CP in place of α4 in HEK293T cells.** HEK293T cells and α4s-FLAG-expressing cells were treated with siRNA against α4 or α6. After 48 h, cells were lysed and subjected to immunoblotting with the indicated antibodies. Data are representative of three independent experiments.

ysis (Fig. 4*C*). In both fractions, the protein level of α6 was comparable between the three cell lines. The protein level of α4 was quite low in α4s-FLAG cells compared with that in mock cells, indicating that peptidase activities observed in α4s-FLAG cells reflect those of α4s-containing CPs but not of cCPs (Fig. 4*C*).

We also assessed the protein-degrading activity of α4s-containing proteasomes by measuring the degradation rate of ornithine decarboxylase. Lysates of α4s-FLAG cells exhibited ornithine decarboxylase-degrading activity comparable with those of other cells (Fig. 4*D*). These results suggest that incorporation of α4s in place of α4 does not affect catalytic activities and specificities of the proteasome.

α4s Is Specifically Expressed in Male Germ Cells—The mammalian testis consists of male germ cells, Sertoli cells, and interstitial cells. To elucidate in which cell type α4s is expressed, cross-sections of adult mouse testes were immunostained using anti-α4s antibody. α4s was detected in the seminiferous tubules (Fig. 5, *A* and *B*, *inside* the *broken line*), whereas no signal of α4s was observed in interstitial cells (Fig. 5, *A* and *B*, *arrowheads*).

The seminiferous tubules contain germ cells and Sertoli cells. To examine whether α4s is expressed in either or both cells, Sertoli cells and germ cells were isolated from the seminiferous tubules, lysed, and subjected to immunoblotting, SOX9 was used as a marker for Sertoli cells (Fig. 5*C*) (20, 21). α4 was expressed in both Sertoli cells and germ cells, whereas α4s was detected only in germ cells but not in Sertoli cells (Fig. 5*C*). These analyses revealed that α4s is specifically expressed in male germ cells.

Expression of α4s Occurs during Meiotic Prophase—Male germ cells undergo a complex process of differentiation called spermatogenesis, in which spermatogonia, germ stem cells, develop into mature sperm. We next examined in which types of germ cells α4s was expressed.

Spermatogenesis proceeds in synchronized waves along the seminiferous tubules, and every given cross-section of the tubule contains only certain cell types in a specific combination. This spermatogenic wave is divided into 12 stages (I to XII) in mice, and germ cells are arranged from the epithelial side to the luminal side of the seminiferous tubules in the order of differentiation (10, 16). Immunohistochemical analysis showed that, in stage I of the seminiferous tubules, α4s was specifically expressed in round spermatids (*RS*) and elongating spermatids (*ES*) but not in early pachytene spermatocytes (*P*) positive for Sycp3, which is known to be expressed in leptotene, zygotene, and pachytene spermatocytes (Fig. 5*A*) (22). In stage VII, on the other hand, α4s was detected in middle pachytene spermatocytes, which are more differentiated than pachytene spermatocytes in stage I (Fig. 5*B*). α4s was also expressed in round spermatids (*RS*) but not in preleptotene spermatocytes (*Pl*) in stage VII (Fig. 5*B*). These results demonstrate that the expression of α4s starts in early to mid-pachytene spermatocytes and continues in spermatids (Fig. 5*D*).

To confirm the temporal expression profile of α4s, we performed further experiments using prepubertal mouse testes. The first spermatogenic wave occurs at around a week after birth, and pachytene spermatocytes and round spermatids first appear at around P14 and P18, respectively, in mice (10). Mouse testes were homogenized and subjected to immunoblot analysis every 2 days from postnatal day 8 (P8) to P18. α4 was constantly expressed in testes on all days (Fig. 5*D*). Sycp3, which exists in two isoforms, was already expressed on P8, whereas the expression of α4s started on P14, suggesting that α4s is expressed after differentiation of germ cells into spermatocytes (Fig. 5*D*) (23).

These developing testes were also subjected to immunostaining (Fig. 5, *E–G*). No obvious signal of α4s was detected in the seminiferous tubules on P10, when the expression of Sycp3 was recognized (Fig. 5*E*). On P14, Sycp3-positive spermatocytes in some cross-sections of the seminiferous tubules (*open arrowheads*) expressed α4s, whereas others (*filled arrowheads*) did not (Fig. 5*F*), similar to adult testes, which contain both α4s-positive and -negative pachytene spermatocytes (Fig. 5, *A* and *B*). On P18, round spermatids were observed that expressed α4s (Fig. 5*G*). These results are consistent with the expression profile of α4s observed in the adult testis. The expression of α4s occurs after the appearance of Sycp3, starts in the Sycp3-positive spermatocytes, and continues in spermatids. Taken together, these results demonstrate that male germ cells express α4s after they enter the meiotic prophase.

The α4s-containing CP Is the Predominant Form of the CP in Mouse Sperm—We next asked whether mature sperm expresses the α4s-containing CP. Glycerol gradient centrifugation analysis of sperm lysates showed that α4s was detected in the CP in mouse sperm (Fig. 6*A*). α4 was also detected in the CP in sperm, indicating that mouse sperm has both α4-containing CPs and α4s-containing CPs (Fig. 6*A*). When the protein levels of α4 and α4s were compared between whole testis lysates and sperm lysates, the amount of α4 relative to α6 was extremely small in sperm lysates compared with that in whole testis lysates (Fig. 6*B*). This result suggests that the expression of the α4-containing CP is severely attenuated in mouse sperm and replaced by the α4s-containing CP.

To estimate how many of the CPs are α4s-containing CPs in mouse sperm, sperm lysates were subjected to immunoprecipitation with either an anti-α6 or anti-α4s antibody, followed by immunoblot analysis of the unbound fractions. Because the anti-α6 antibody immunoprecipitates all types of CPs, the unbound fraction contained neither α4s nor α6 (Fig. 6*C*). The anti-α4s antibody immunoprecipitates α4s-containing CPs, whereas it does not immunoprecipitate α4-containg CPs. Indeed, α4s was

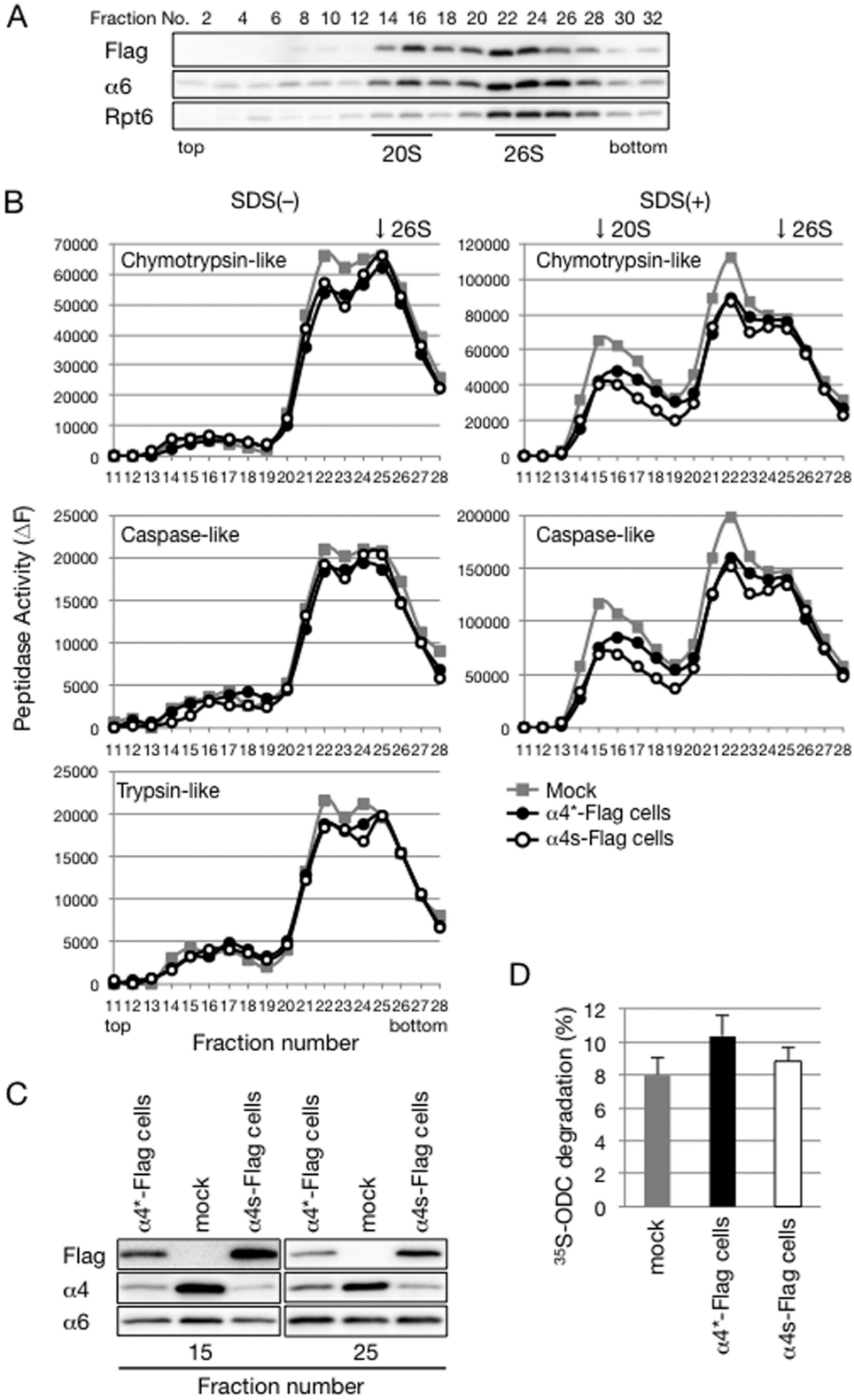

FIGURE 4. **Incorporation of α4s does not alter the catalytic activities of the proteasome.** *A*, extracts of HEK293T cells expressing both α4s-FLAG and α4-shRNA (α4s-FLAG cells) were fractionated by glycerol gradient centrifugation and subjected to immunoblotting with the indicated antibodies. *B*, lysates of α4s-FLAG cells, α4*-FLAG cells, and mock HEK293T cells were fractionated by glycerol gradient centrifugation, and the peptidase activities of each fraction were measured in the absence (*left*) and presence (*right*) of 0.025% SDS. *Arrows* indicate the peak locations of 20 S CPs and 26 S proteasomes. *C*, fractions 15 and 25 in *B* were subjected to immunoblotting for the indicated antibodies. Data are representative of three independent experiments (*A*–*C*). *D*, cell extracts of these three cell lines were assayed for ATP-dependent protein degradation activity using ^{35}S-labeled ornithine decarboxylase as a substrate. Mean ± S.D. ($n = 3$).

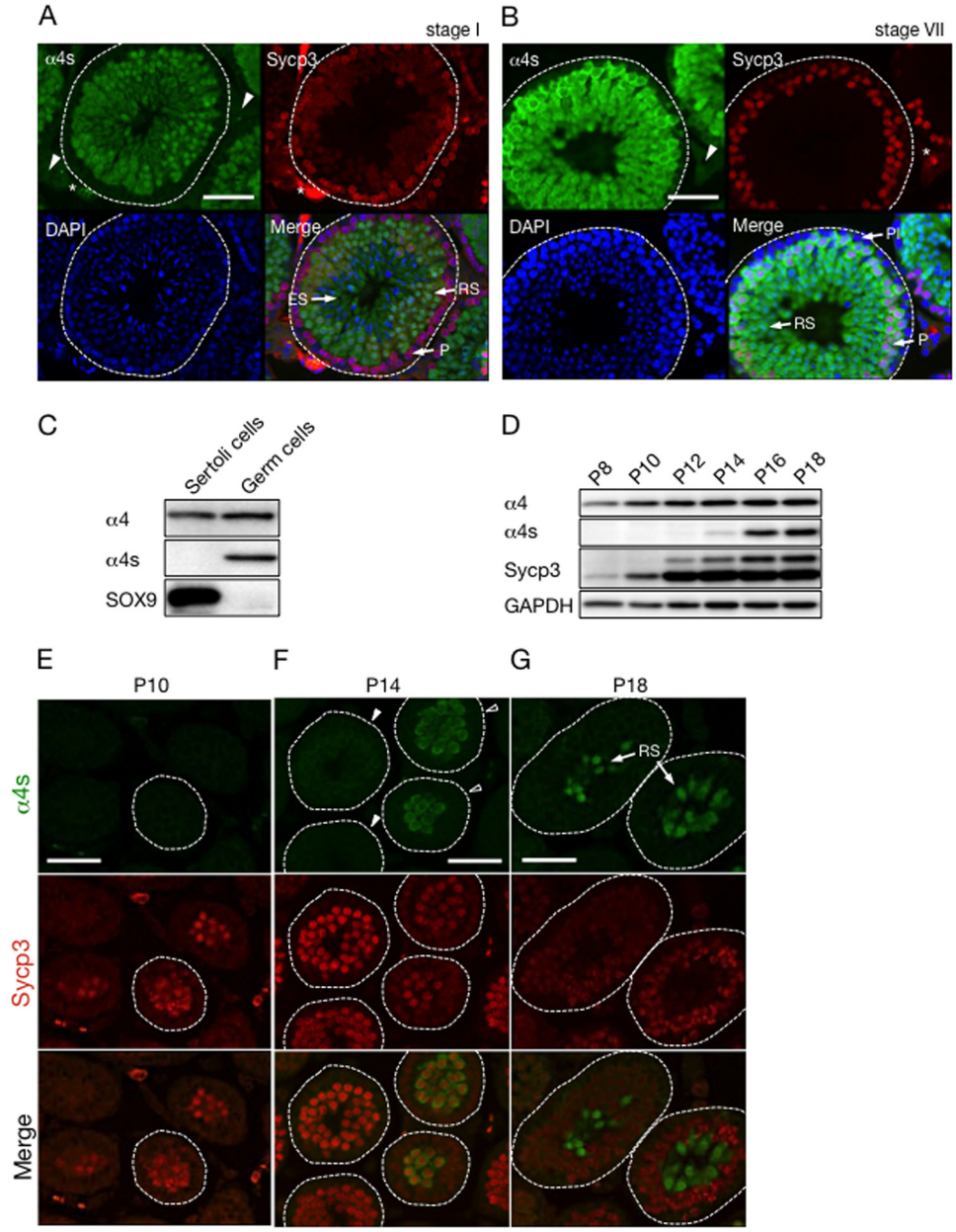

FIGURE 5. **α4s is specifically expressed in meiotic and postmeiotic male germ cells.** *A* and *B*, cross-sections of seminiferous tubules in stage I (*A*) and stage VII (*B*) from adult mice were stained with anti-α4s antibody (*green*), anti-Sycp3 antibody (*red*), and DAPI (*blue*). *White broken lines*, the edge of seminiferous tubules; *arrowheads*, interstitial cells; *asterisks*, nonspecific signals; *Pl*, preleptotene spermatocyte; *P*, pachytene spermatocyte; *RS*, round spermatid; *ES*, elongating spermatid. *Scale bar* = 50 μm. *C*, Sertoli cells and germ cells were isolated and subjected to immunoblotting with the indicated antibodies. *D*, expression of α4s in the testis during mouse postnatal development was analyzed by immunoblotting. GPADH was used as a control. *Asterisk*, nonspecific bands. Data are representative of two independent experiments. *E–G*, the cross-sections of developing testes in *D* were immunostained with anti-α4s antibody (*green*) and anti-Sycp3 antibody (*red*). The *open* and *filled arrowheads* indicate the seminiferous tubules in which α4s was detected and not detected, respectively. *White broken lines* denote the edges of seminiferous tubules. *Scale bars* = 50 μm.

depleted by immunoprecipitation with the anti-α4s-antibody. The anti-α4s antibody also depleted the majority of α6, although a small amount of α6 remained in the unbound fraction (Fig. 6*C*). This suggests that the majority of the CP in the sperm is α4s-containig CPs.

To confirm this observation, the immunoprecipitates with the anti-α6 antibody were serially diluted and compared with the amount of α6 in the immunoprecipitates with anti-α4s antibody. This indicates that ~80% of the CPs in sperm lysates contain α4s (Fig. 6*D*). Therefore, we concluded that most of the CPs in the mouse sperm are α4s-containg CPs.

Ubiquitin-Proteasome Mediated Protein Degradation Occurs in Mature Sperm—During mammalian spermatogenesis, most parts of the cytoplasm are removed from spermatids to acquire the shape of mature sperm (24, 25). It is intriguing to ask whether the proteasome is still working in mature sperm cells. To examine this, mouse sperm was treated with epoxomicin, a proteasome inhibitor, and lysed for immunoblot analysis with anti-ubiquitin antibody (Fig. 6*E*) (26). Incubation of sperm with epoxomicin caused accumulation of ubiquitinated proteins, suggesting that degradation of ubiquitinated proteins by the proteasome is occurring in mouse sperm (Fig. 6*E*).

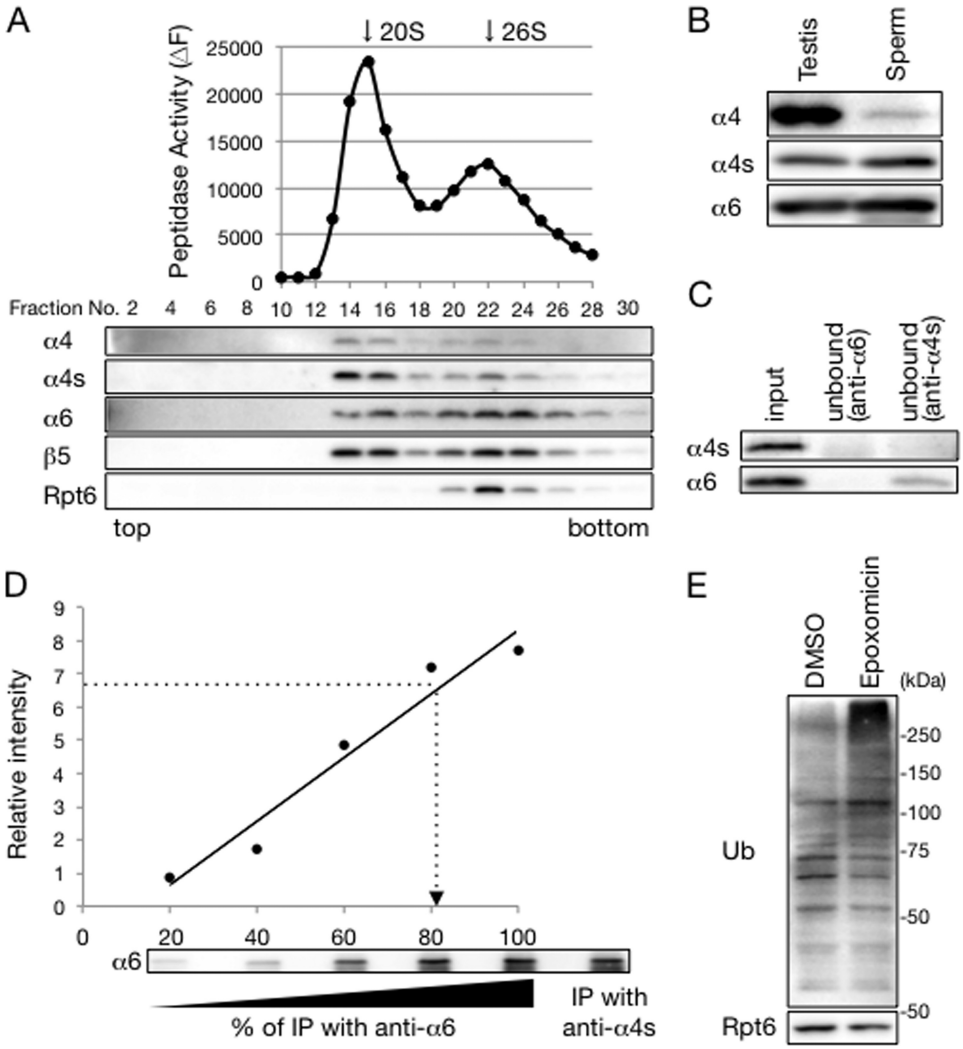

FIGURE 6. **The α4s-containing CP is the predominant form of CP in mature sperm.** *A*, extracts of adult mouse sperm were fractionated by glycerol gradient centrifugation. The chymotrypsin-like activity of the resultant fractions was measured in the presence of 0.025% SDS (*top panel*). *Arrows* indicate the peak locations of the 20 S CP and the 26 S proteasome. Each fraction was subjected to immunoblotting with the indicated antibodies (*bottom panel*). *B*, extracts of adult mouse testes and sperm were subjected to immunoblotting with the indicated antibodies. *C*, equal amounts of mouse sperm extracts (*input*) were immunoprecipitated with either anti-α6 antibody or anti-α4s antibody. The resultant unbound fractions as well as the input were subjected to immunoblotting with the indicated antibodies. *D*, immunoprecipitates (*IP*) with anti-α6 antibody were serially diluted (20, 40, 60, 80, and 100%) and subjected to immunoblotting for α6. Each band was quantified by densitometry and used to generate a standard curve for estimation of the amount of α6. The band of α6 in the immunoprecipitate with anti-α4s antibody was quantified following estimation of its amount by interpolation on the standard curve (*dotted line*). *E*, mouse sperm was incubated with dimethyl sulfoxide (*DMSO*) or 10 μM epoxomicin for 7 h and lysed for immunoblot analysis with antibodies against ubiquitin (*Ub*) and Rpt6 . Data in are representative of at least three independent experiments.

DISCUSSION

A recent study by Qian *et al.* (9) first reported a newly found α-type subunit expressed in the mammalian male germ cell. This subunit, referred to as α4s, has high homology to α4 and was included in proteasomes purified from mammalian testes (Fig. 1) . However, the subunit composition of the α4s-containing proteasome has not yet been examined. In this study, we further characterized α4s and the α4s-containing proteasome in detail.

Qian *et al.* (9) showed that α4s is specifically expressed in spermatids and sperm but not in spermatocytes and spermatogonia . However, our analysis of developing testes as well as observation of adult seminiferous tubules in various stages showed that expression of α4s starts at an earlier stage of spermatogenesis and that spermatocytes also express α4s after they enter the meiotic prophase (Fig. 5).

Our biochemical analysis clarified that α4s is incorporated into the CP in place of α4 (Figs. 2 and 3). The CP is formed by dimerization of two half-CPs that have one α ring and one β ring, and, thus, the CP has two α rings (27). Although both α4 and α4s are expressed in germ cells, CPs possessing both α4 and α4s do not seem to be present in the testis, which is revealed by immunoprecipitation by an antibody specific to α4s, that we generated in this study (Fig. 2*C*). We also showed that α4s-containing CPs do not include catalytic β subunits of iCPs, although mammalian testes express these subunits (Fig. 2*C*). These findings suggest a specific mechanism by which assembly of the α4s-containing CP is regulated (11, 27).

Comparison of the structural models of α4 and α4s showed that differences between the two subunits are located on the outer surfaces of the CP (Fig. 1). α4 is reported to directly interact with various molecules, such as Rab7, mitochondrial antivi-

ral signaling protein (MAVS), c-Abl, and HIF-1α (28–31). These molecules are likely to interact with residues of α4 that are exposed to the outer surface of the CP. Analogous to α4, it is possible that α4s interacts with some molecules distinct from the α4-interacting molecules in male germ cells, which might confer specific roles on the α4s-containing CP.

Qian *et al.* (9) showed that "spermatoproteasomes," which designates PA200-associated proteasomes in the testis, are required for the degradation of acetylated histones during spermatogenesis . Although they showed that PA200 is essential for this function, the physiological role of α4s is still totally unknown. Our immunoblot analysis using sperm lysates showed that incubation of sperm with a proteasome inhibitor caused accumulation of ubiquitinated proteins (Fig. 6*E*). Considering that the majority of the CPs in mouse sperm is α4s-containing proteasomes (Fig. 6, *A–D*), these results suggest that sperm has substrates that are ubiquitinated and sequentially degraded by α4s-containing proteasomes. Identification of such substrate proteins might give a clue to understand the role of α4s in the future.

Acknowledgment—We thank Larissa Kogleck for advice and comments regarding the manuscript.

REFERENCES

1. Glickman, M. H., and Ciechanover, A. (2002) The ubiquitin-proteasome proteolytic pathway: destruction for the sake of construction. *Physiol. Rev.* **82,** 373–428
2. Ravid, T., and Hochstrasser, M. (2008) Diversity of degradation signals in the ubiquitin-proteasome system. *Nat. Rev. Mol. Cell Biol.* **9,** 679–690
3. Schwartz, A. L., and Ciechanover, A. (2009) Targeting proteins for destruction by the ubiquitin system: implications for human pathobiology. *Annu. Rev. Pharmacol. Toxicol.* **49,** 73–96
4. Murata, S., Yashiroda, H., and Tanaka, K. (2009) Molecular mechanisms of proteasome assembly. *Nat. Rev. Mol. Cell Biol.* **10,** 104–115
5. Coux, O., Tanaka, K., and Goldberg, A. (1996) Structure and functions of the 20 S and 26 S proteasomes. *Annu. Rev. Biochem.* **65,** 801–847
6. Takahama, Y., Takada, K., Murata, S., and Tanaka, K. (2012) β5t-containing thymoproteasome: specific expression in thymic cortical epithelial cells and role in positive selection of $CD8^+$ T cells. *Curr. Opin. Immunol.* **24,** 92–98
7. Tanaka, K., and Kasahara, M. (1998) The MHC class I ligand-generating system: roles of immunoproteasomes and the interferon-γ-inducible proteasome activator PA28. *Immunol. Rev.* **163,** 161–176
8. Murata, S., Sasaki, K., Kishimoto, T., Niwa, S., Hayashi, H., Takahama, Y., and Tanaka, K. (2007) Regulation of $CD8^+$ T cell development by thymus-specific proteasomes. *Science* **316,** 1349–1353
9. Qian, M.-X., Pang, Y., Liu, C. H., Haratake, K., Du, B.-Y., Ji, D.-Y., Wang, G.-F., Zhu, Q.-Q., Song, W., Yu, Y., Zhang, X. X., Huang, H. T., Miao, S., Chen, L. B., Zhang, Z. H., Liang, Y. N., Liu, S., Cha, H., Yang, D., Zhai, Y., Komatsu, T., Tsuruta, F., Li, H., Cao, C., Li, W., Li, G. H., Cheng, Y., Chiba, T., Wang, L., Goldberg, A. L., Shen, Y., and Qiu, X. B. (2013) Acetylation-mediated proteasomal degradation of core histones during DNA repair and spermatogenesis. *Cell* **153,** 1012–1024
10. Bellvé, A. (1993) Purification, culture, and fractionation of spermatogenic cells. *Methods Enzymol.* **225,** 84–113
11. Hirano, Y., Hayashi, H., Iemura, S., Hendil, K. B., Niwa, S., Kishimoto, T., Kasahara, M., Natsume, T., Tanaka, K., and Murata, S. (2006) Cooperation of multiple chaperones required for the assembly of mammalian 20 S proteasomes. *Mol. Cell* **24,** 977–984
12. Kaneko, T., Hamazaki, J., Iemura, S., Sasaki, K., Furuyama, K., Natsume, T., Tanaka, K., and Murata, S. (2009) Assembly pathway of the mammalian proteasome base subcomplex is mediated by multiple specific chaperones. *Cell* **137,** 914–925
13. Tanahashi, N., Murakami, Y., Minami, Y., Shimbara, N., Hendil, K. B., and Tanaka, K. (2000) Hybrid proteasomes. Induction by interferon-γ and contribution to ATP-dependent proteolysis. *J. Biol. Chem.* **275,** 14336–14345
14. Hamazaki, J., Iemura, S., Natsume, T., Yashiroda, H., Tanaka, K., and Murata, S. (2006) A novel proteasome interacting protein recruits the deubiquitinating enzyme UCH37 to 26 S proteasomes. *EMBO J.* **25,** 4524–4536
15. Tajima, Y., Onoue, H., Kitamura, Y., and Nishimune, Y. (1991) Biologically active kit ligand growth factor is produced by mouse Sertoli cells and is defective in SId mutant mice. *Development* **113,** 1031–1035
16. Russell, L. D., Ettlin, R., Hikim, A. P. S., and Clegg, E. D. (1990) *Histological and Histopathological Evaluation of the Testis*, pp. 41–48 and 119–161, Cache River Press, Clearwater, FL
17. Unno, M., Mizushima, T., Morimoto, Y., Tomisugi, Y., Tanaka, K., Yasuoka, N., and Tsukihara, T. (2002) The structure of the mammalian 20 S proteasome at 2.75 resolution. *Structure* **10,** 609–618
18. Arnold, K., Bordoli, L., Kopp, J., and Schwede, T. (2006) The SWISS-MODEL workspace: a web-based environment for protein structure homology modelling. *Bioinformatics* **22,** 195–201
19. Ustrell, V., Hoffman, L., Pratt, G., and Rechsteiner, M. (2002) PA200, a nuclear proteasome activator involved in DNA repair. *EMBO J.* **21,** 3516–3525
20. Gao, F., Maiti, S., Alam, N., Zhang, Z., Deng, J. M., Behringer, R. R., Lécureuil, C., Guillou, F., and Huff, V. (2006) The Wilms tumor gene, Wt1, is required for Sox9 expression and maintenance of tubular architecture in the developing testis. *Proc. Natl. Acad. Sci.* **103,** 11987–11992
21. Kent, J., Wheatley, S. C., Andrews, J. E., Sinclair, A. H., and Koopman, P. (1996) A male-specific role for SOX9 in vertebrate sex determination. *Development* **122,** 2813–2822
22. Yuan, L., Liu, J. G., Zhao, J., Brundell, E., Daneholt, B., and Höög, C. (2000) The murine SCP3 gene is required for synaptonemal complex assembly, chromosome synapsis, and male fertility. *Mol. Cell* **5,** 73–83
23. Alsheimer, M., Baier, A., and Schramm, S. (2010) Synaptonemal complex protein SYCP3 exists in two isoforms showing different conservation in mammalian evolution. *Cytogenet. Genome Res.* **128,** 162–168
24. Breucker, H., Schäfer, E., and Holstein, A.-F. (1985) Morphogenesis and fate of the residual body in human spermiogenesis. *Cell Tissue Res.* **240,** 303–309
25. Blanco-Rodríguez, J., and Martínez-García, C. (1999) Apoptosis is physiologically restricted to a specialized cytoplasmic compartment in rat spermatids. *Biol. Reprod.* **61,** 1541–1547
26. Meng, L., Mohan, R., Kwok, B. H., Elofsson, M., Sin, N., and Crews, C. M. (1999) Epoxomicin, a potent and selective proteasome inhibitor, exhibits *in vivo* antiinflammatory activity. *Proc. Natl. Acad. Sci.* **96,** 10403–10408
27. Hirano, Y., Hendil, K. B., Yashiroda, H., Iemura, S., Nagane, R., Hioki, Y., Natsume, T., Tanaka, K., and Murata, S. (2005) A heterodimeric complex that promotes the assembly of mammalian 20 S proteasomes. *Nature* **437,** 1381–1385
28. Montagner, M., Enzo, E., Forcato, M., Zanconato, F., Parenti, A., Rampazzo, E., Basso, G., Leo, G., Rosato, A., and Bicciato, S. (2012) SHARP1 suppresses breast cancer metastasis by promoting degradation of hypoxia-inducible factors. *Nature* **487,** 380–384
29. Dong, J., Chen, W., Welford, A., and Wandinger-Ness, A. (2004) The proteasome α-subunit XAPC7 interacts specifically with Rab7 and late endosomes. *J. Biol. Chem.* **279,** 21334–21342
30. Liu, X., Huang, W., Li, C., Li, P., Yuan, J., Li, X., Qiu, X. B., Ma, Q., and Cao, C. (2006) Interaction between c-Abl and Arg tyrosine kinases and proteasome subunit PSMA7 regulates proteasome degradation. *Mol. Cell* **22,** 317–327
31. Jia, Y., Song, T., Wei, C., Ni, C., Zheng, Z., Xu, Q., Ma, H., Li, L., Zhang, Y., and He, X. (2009) Negative regulation of MAVS-mediated innate immune response by PSMA7. *J. Immunol.* **183,** 4241–4248